# Paper Pentasia: An Aperiodic Surface in Modular Origami

Robert J. Lang[a*] and Barry Hayes[b†]
[a]*Langorigami.com, Alamo, California, USA,*
[b]*Stanford University, Stanford, CA*

2013-05-26

Origami, the Japanese art of paper-folding, has numerous connections to mathematics, but some of the most direct appear in the genre of *modular origami*. In modular origami, one folds many sheets into identical units (or a few types of unit), and then fits the units together into larger constructions, most often, some polyhedral form. Modular origami is a diverse and dynamic field, with many practitioners (see, e.g., [12, 3]). While most modular origami is created primarily for its artistic or decorative value, it can be used effectively in mathematics education to provide physical models of geometric forms ranging from the Platonic solids to 900-unit pentagon-hexagon-heptagon torii [5].

As mathematicians have expanded their catalog of interesting solids and surfaces, origami designers have followed not far behind, rendering mathematical forms via folding, a notable recent example being a level-3 Menger Sponge folded from 66,048 business cards by Jeannine Mosely and co-workers [10]. In some cases, the origami explorations themselves can lead to new mathematical structures and/or insights. Mosely's developments of business-card modulars led to the discovery of a new fractal polyhedron with a novel connection to the famous Snowflake curve [11].

One of the most popular geometric mathematical objects has been the sets of aperiodic tilings developed by Roger Penrose [14, 15], which acquired new significance with the discovery of quasi-crystals, their three-dimensional analogs in the physical world, in 1982 by Daniel Schechtman, who was awarded the 2011 Nobel Prize in Chemistry for his discovery. Penrose tilings, both kite-dart and rhomb tilings, have found application in a wide variety of decorative arts, as both purely 2D (flat) tilings, as well as quasi-three-dimensional structures, which are based on a 2D tiling but add some form of surface relief in the third dimension, for example, Anne Preston's 2000 sculpture "You Were in Heaven," installed at San Francisco International Airport [16].

Aperiodic tilings in general and Penrose tilings in particular seem like a natural fit to

*Corresponding author. Email: robert@langorigami.com
†Email: bhayes@gmail.com

modular origami. It is surprising, then, that to our knowledge, there is no published example of origami modules that tile aperiodically. In this paper, we aim to rectify this omission.

In this paper, we present a set of two origami modular units that when combined with multiple copies of themselves, create a polyhedral surface that is aperiodic; it is, in fact, based upon the Penrose kite-dart tiling. The surface thereby formed, titled *Pentasia*, was described by John H. Conway in a symposium over 10 years ago but has not been previously described in print. It is remarkable in that despite the strong 5-fold symmetry and appearance of the golden ratio, it is composed entirely of equilateral triangles. In this paper, we describe the construction of the aperiodic Pentasia surface and a related surface based on the Penrose rhomb tiling (also not previously described). We then construct its realization by origami units, and conclude with some observations about the surface itself and further avenues for both mathematical and origamical explorations.

## Penrose Tilings

The Penrose tiles, introduced to a popular audience by Martin Gardner [4], have been widely discussed and analyzed, so we will provide a quick recap here, following De Bruijn [1] and adopting notation introduced in Lyman Hurd's *Mathematica*™ package, *PenroseTiles* [6]. There are two tiles, known as the "kite" and the "dart," illustrated in Figure 1, which, when certain edge-matching conditions are satisfied, tile the plane aperiodically, as illustrated in Figure 1.

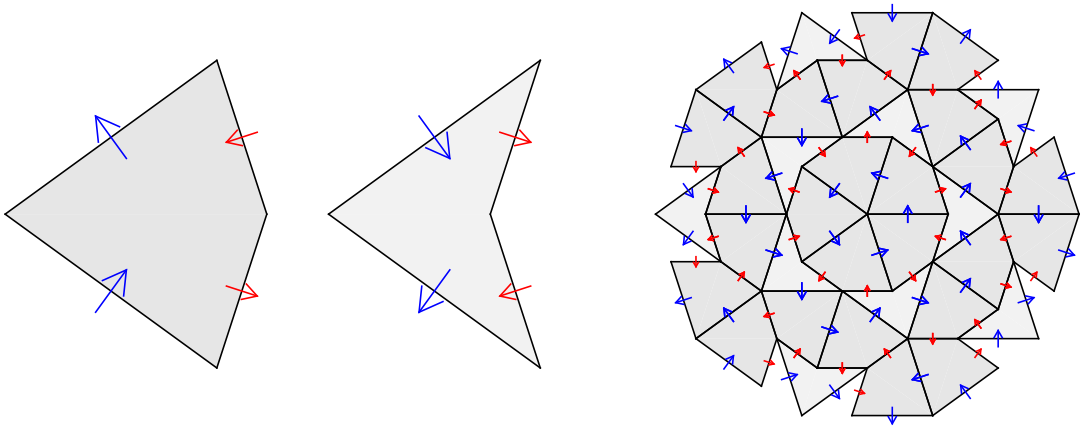

Figure 1: Left: the kite and dart. Right: a portion of a kite-dart tiling.

A closely related second tiling is the Penrose rhomb tiling, illustrated in Figure 2. In this tiling, copies of two rhombii (which are commonly called the "skinny rhomb" and the "fat rhomb") are tiled, again, with certain edge-matching conditions. For both tilings, the matching conditions may be enforced in a variety of ways, e.g., by marking arrows along the edges or decorating the tiles with curved lines. We have chosen a set of colored arrows

that cross the edges (for reasons that will shortly become apparent). The rules for both types of tiling are that two edges can meet only if their corresponding arrows match in both color and direction. The arrows enforce conditions so that among the eight edges of the two quadrilateral tiles, for any given edge, there are only two edges that can mate with the given one.

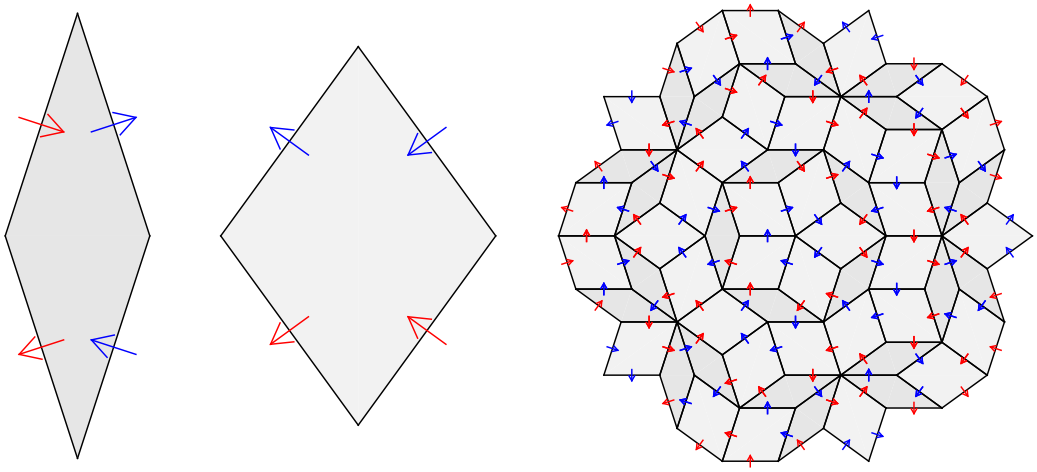

Figure 2: Left: the fat and skinny rhombs. Right: a portion of a rhomb tiling.

While one may construct a Penrose tiling by assembling individual tiles while obeying the matching rules, the matching rules are not sufficient to guarantee an arbitrarily large tiling; it is possible to construct a partial tiling that obeys the matching rules, but that possesses a hole that cannot be filled by any combination of the tiles. It is possible, however, to construct arbitrarily large patterns using the process known as *deflation*. Deflation takes a given tiling and constructs a finer-grained version with a larger number of tiles. Deflation also provides an elegant illustration of the relationship between the kite-dart and rhomb tilings.

To deflate a Penrose tiling, we divide each quadrilateral—kite, dart, or rhomb—into two mirror-image triangles, as shown in Figure 3. The kite and skinny rhomb are both divided into two acute isoceles triangles with a tip angle of 36° and whose sides are in the golden ratio, $\phi \equiv (1+\sqrt{5})/2$. Similarly, the dart and fat rhomb are both divided into two obtuse isoceles triangles with a tip angle of 108°; they, too have their sides in the golden ratio. We note, though, that within a given tiling, the relative sizes of the acute and isoceles triangles are different: in kite-dart tiles, acute triangles are larger than obtuse, while in rhomb tilings, obtuse triangles are larger than acute.[1]

Let us denote an acute triangle of a kite tile by $a_1(x, y, z)$, where $x = (x_1, x_2)$, $y = (y_1, y_2)$, and $z = (z_1, z_2)$ are the 2D coordinates of its vertices. Thus, a kite tile is made up of two $a_1$

[1]The terminology of "deflation" and "inflation" has evolved over time; the term "decomposition" is now more commonly used for this process.

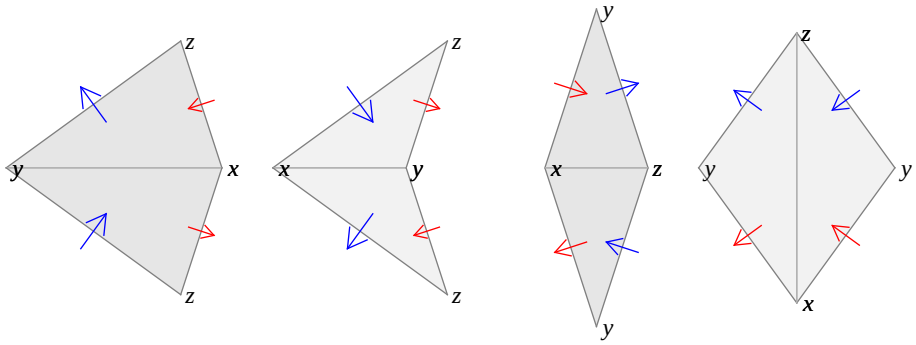


Figure 3: Kite, dart, skinny rhomb, and fat rhomb, divided into acute and obtuse triangle pairs.

triangles where one is the reflection of the other in its $(x, z)$ edge. Similarly, let us denote an obtuse triangle of a dart tile by $o_1(x, y, z)$, so that a dart tile is made up of two $o_1$ triangles. And in the same fashion, we will denote the acute triangle of a skinny rhomb tile by $a_2(x, y, z)$ and the obtuse triangle of a fat rhomb tile by $o_2(x, y, z)$. Each tile consists of two mirror-image triangles in which the matching arrow directions are reversed in the mirror image tile. To properly account for arrow reversal in the mirror-image triangles, the arrow directions are not defined as incoming or outgoing, but rather as a rotation of the edge direction: in the acute kite triangle, for example, the red arrows are a 90° CCW rotation of the vector from $x$ to $z$, and so forth, for the other edges of other triangles.

Deflation is the process of dissecting each of the triangles into smaller versions of the same triangles. The process of deflation can be described by a set of production rules akin to those of Lindenmeyer systems[17], expressed as follows:

$$\begin{aligned} a_1(x,y,z) &\mapsto \{a_2(\tfrac{1}{\phi}x + \tfrac{1}{\phi^2}y, z, x), o_2(z, \tfrac{1}{\phi}x + \tfrac{1}{\phi^2}y, y)\}, \\ o_1(x,y,z) &\mapsto \{o_2(x,y,z)\}, \\ a_2(x,y,z) &\mapsto \{a_1(x,y,z)\}, \\ o_2(x,y,z) &\mapsto \{a_1(y,x,\tfrac{1}{\phi^2}x + \tfrac{1}{\phi}z), o_1(z, \tfrac{1}{\phi^2}x + \tfrac{1}{\phi}z, y)\}. \end{aligned} \tag{1}$$

Figure 4 shows the deflation operation applied to the four types of triangle. Here we have left off drawing the side of each triangle along which it mates with a mirror image triangle to form a tile.

The process of deflation ensures that matching rules are satisfied at each stage and that acute and obtuse triangles always appear in pairs that can be reassembled into the kite and dart tiles (with the exception of some unpaired triangles, i.e., half-tiles, that may be found along the boundary of the pattern). Successive steps of deflation alternate between kite-dart and rhomb tilings.

Deflation can be applied to any valid Penrose kite-dart tiling to transform it into a finer-grained tiling that is also guaranteed to be valid.

Any finite patch of a Penrose tiling appears an infinite number of times in the infinite aperiodic tiling, but there are two special families of finite tiling patches that have perfect

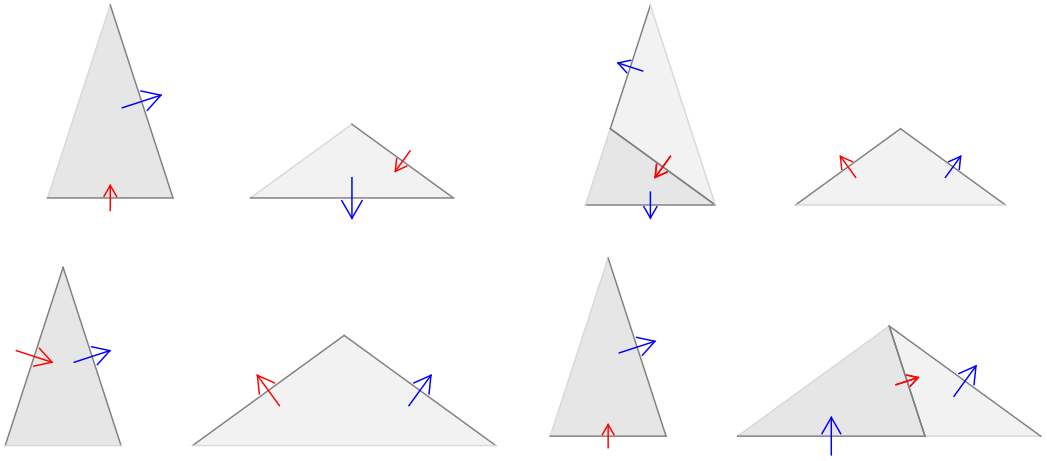

Figure 4: Top left: acute ($a_1$) and obtuse ($o_1$) triangles from a kite and dart. Top right: the same after deflation, consisting of $a_2$ and $o_2$ triangles. Bottom left: acute ($a_2$) and obtuse ($o_2$) triangles from the rhombs. Bottom right: the same after deflation, consisting of $a_1$ and $o_1$ triangles.

fivefold symmetry. Each family can be constructed by successive deflations of two basic patterns, known as the "Sun" and "Star," which are illustrated in Figures 5 and 6.

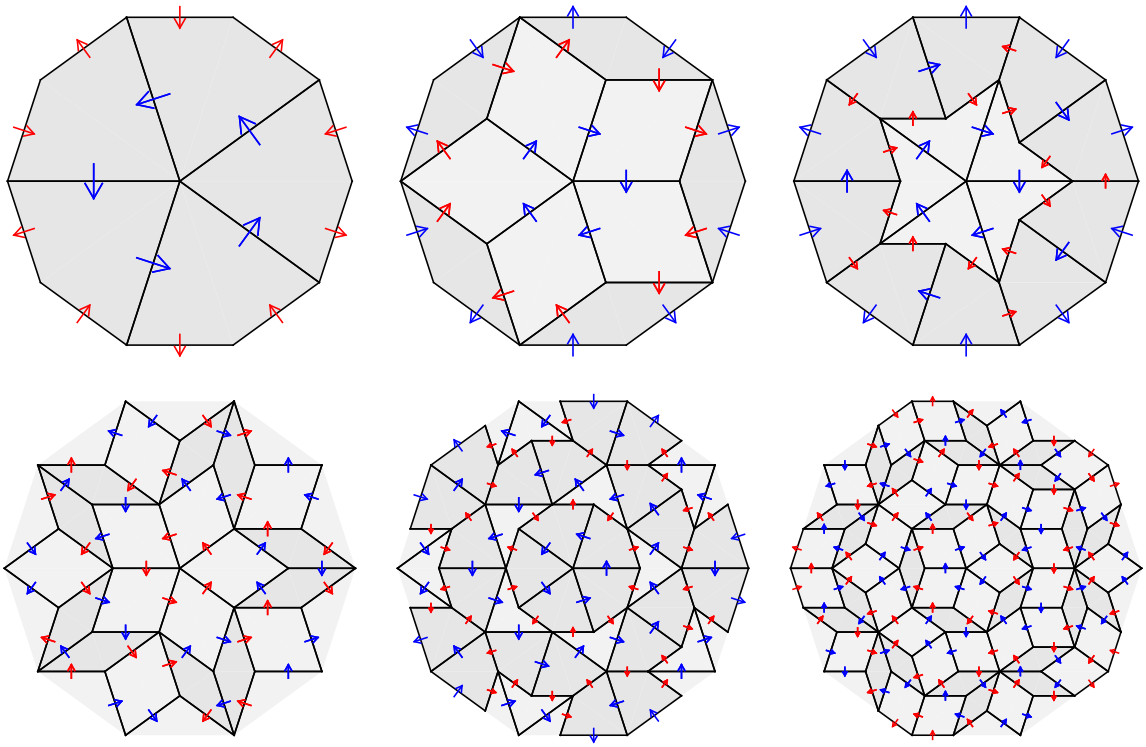

Figure 5: Successive deflations of the Sun.

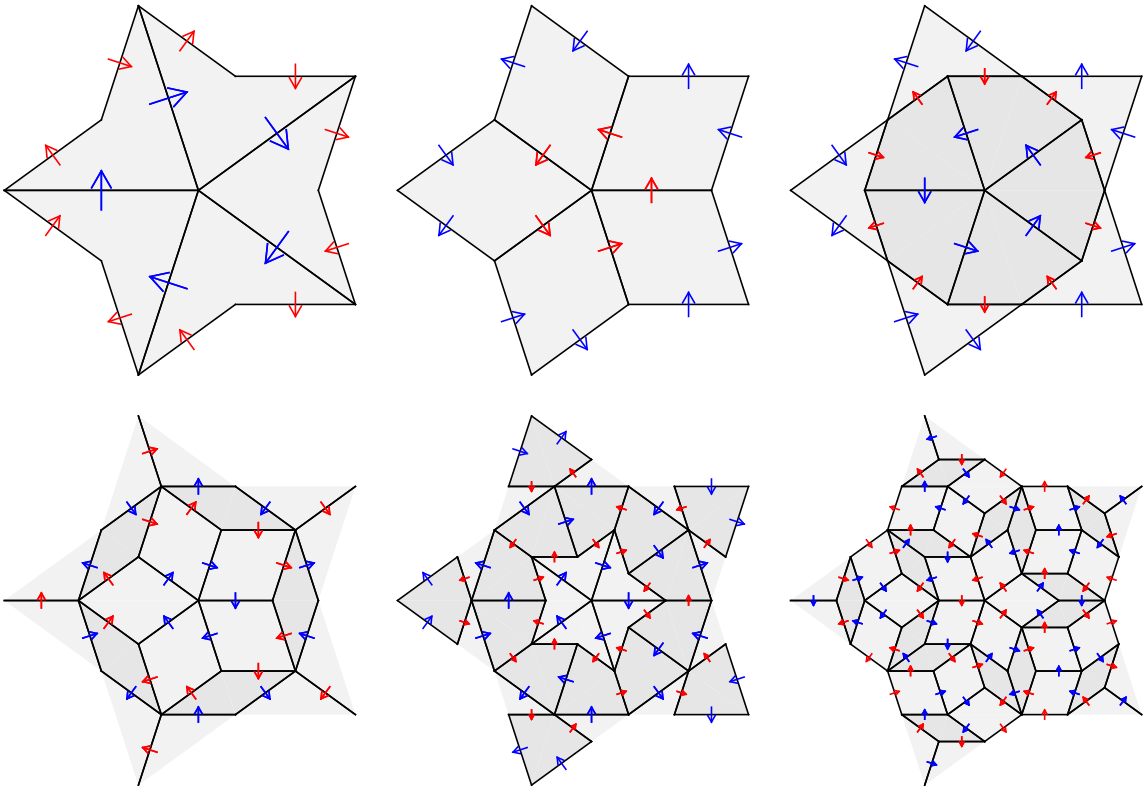

Figure 6: Successive deflations of the Star.

Recursive deflations of either the Sun or Star results in successively larger Penrose tilings, all of which maintain the fivefold symmetry of the initial figure. Note that the first deflation of the Sun and Star both produce a star of fat rhombs in the center, but they differ in which matching arrows are central. This difference forces the next set of skinny rhombs to have different orientations for the two types of rhomb stars, leading to fundamentally different arrangements of subsequent tiles.

# Pentasia

In 2002, one author [RJL] saw a presentation by John H. Conway[2] in which he pointed out that one could create a surface in $\mathbb{R}^3$ composed of equilateral triangles from a kite-dart Penrose tiling, in which each of the kite and dart quadrilaterals in the plane is replaced by a pair of equilateral triangles that are joined along one edge into a folded quadrilateral. To our knowledge[3], this surface has not been previously described in print; we do so now.

For each planar tile, we create a 3D pair of triangles joined along one edge. The quadrilateral formed by each folded pair is oriented so that the projection into the plane of the

[2]In an impromptu lecture given at the conference *Gathering for Gardner 5*, Atlanta, Ga., April 5–7, 2002.
[3]and Conway's

remaining unpaired edges is aligned precisely with the edges of their corresponding tile. The triangle pairs can be divided into two classes: "kite-like" pairs whose projection is a kite, and "dart-like" pairs whose projection is a dart. In the case of the kite-like pair, its true shadow is a kite; for the dart-like pair, because of the overhang, the shadow of the solid triangles is not a dart, but the shadow of the four exterior edges matches the dart. Figure 7 shows examples of both the kite and dart triangle pairs in 3D.

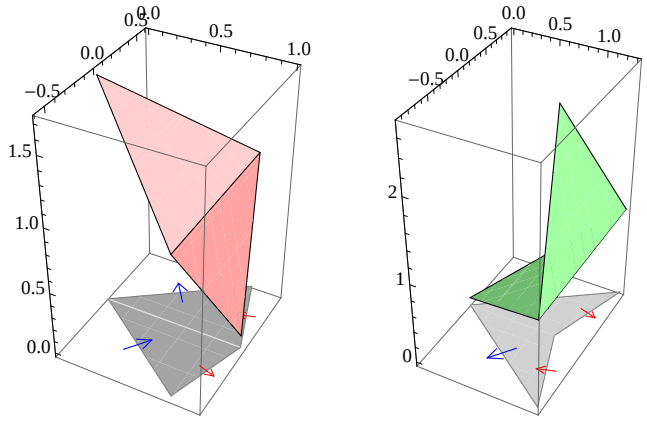


Figure 7: Left: a kite-like triangle pair above a kite tile. Right: a dart-like triangle pair above a dart tile.

Note that the reflex corner of the dart is the shadow cast by the highest point of the dart-like triangle pair.

Somewhat remarkably, these folded pairs of triangles can be arranged (via translation and/or rotation about a vertical axis) so that they mate with each other edge-to-edge in 3D in the same way that the Penrose tiles meet up in the plane, forming a continuous, unbroken surface. Conway has dubbed this surface "Pentasia." Two examples of Pentasia are illustrated in Figure 8 above their respective planar tilings.

The fivefold-symmetric tiling with a Sun at the center reaches its maximum altitude above the Sun, topped off with (most of) an icosahedron. Conway called this region of Pentasia the "Temple of the Sun." Conversely, the fivefold symmetric tiling with a Star at its center reaches its minimum altitude above the center; this is the "Star Lake." The extended surface contains numerous partial copies of the Temple and Lake at varying elevation.

Recall that planar tiles could be divided into two mirror-image triangles, $a_1$ and $o_1$, respectively. In the same fashion, we can divide each 3D triangle pair into two half-triangles (which are, of course, still triangles), for a total of four half-triangles per tile, or two half-triangles for each of the planar triangles.

For a given planar tile, the edge lengths and orientations of its elevated triangles are fixed; the only free variable is the height $h$ above the plane, which we arbitrarily choose to be the height of the horizontal fold line, normalized to the length of a side of its corresponding triangle ($x - z$ for acute triangles, $x - y$ for obtuse triangles). Thus, we can fully specify each pair of half-triangles by the coordinates of its corresponding planar triangle, plus the height

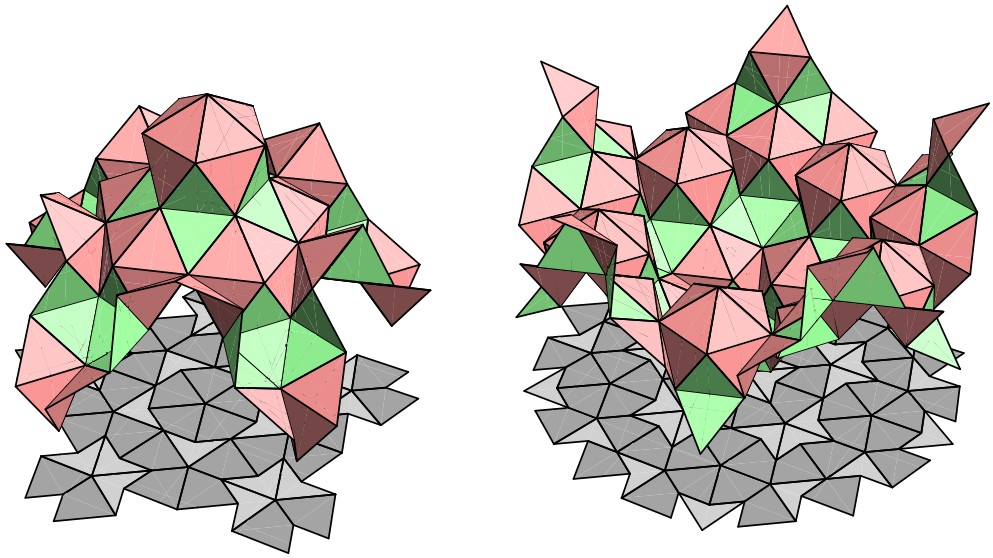

Figure 8: Left: the Temple of the Sun. Right: the Star Lake.

parameter $h$ of the fold line. We denote this information by $a_3(x, y, z, h)$ and $o_3(x, y, z, h)$, respectively, as illustrated for acute and obtuse planar triangles in Figure 9.

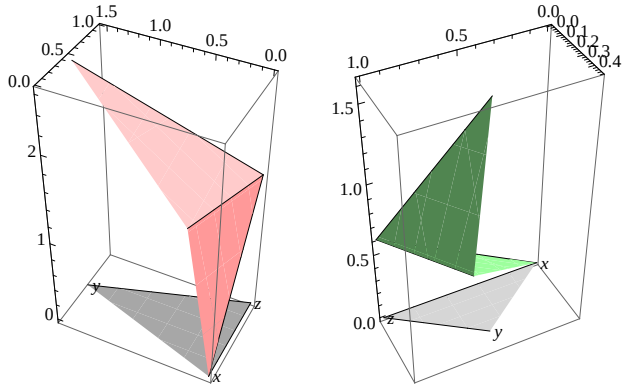


Figure 9: Left: Planar acute triangle $a_1(x, y, z)$ and the 3D triangle pair with specifier $a_3(x, y, z, \phi)$. Right: Planar obtuse triangle $o_1(x, y, z)$ and the 3D triangle pair with specifier $o_3(x, y, z, \phi - 1)$.

Note that coordinates $x, y, z$ are 2D planar coordinates, not the 3D vertices of the two elevated half-triangles, which are both $30°/60°/90°$ right triangles, joined along their shared

short edges. The four vertices of the two triangles can be constructed from the 2D coordinates $x = (x_1, x_2), y = (y_1, y_2), z = (z_1, z_2)$ and the height parameter $h$ of the acute and obtuse triangles as follows.

For the acute triangle $a_3(x, y, z, h)$, we define four vertices

$$\begin{array}{rcl} x' & = & (x_1, x_2, |x - z|(h - \phi)), \\ y' & = & (y_1, y_2, |x - z|(h + 1)), \\ z' & = & (z_1, z_2, |x - z|(h)), \\ w' & = & (\frac{\phi}{2}x_1 + (1 - \frac{\phi}{2})y_1, \frac{\phi}{2}x_2 + (1 - \frac{\phi}{2})y_2, |x - z|(h)). \end{array} \tag{2}$$

Then the two half-triangles are given by $\triangle(x', w', z')$ and $\triangle(z', w', y')$, sharing side $(w', z')$.

In the same way, for the obtuse triangle $o_3(x, y, z, h)$, we define the four vertices

$$\begin{array}{rcl} x' & = & (x_1, x_2, |x - y|(h - 1)), \\ y' & = & (y_1, y_2, |x - y|(h + \phi)), \\ z' & = & (z_1, z_2, |x - y|(h)), \\ w' & = & (\frac{-1}{2\phi}x_1 + \frac{\phi^2}{2}y_1, \frac{-1}{2\phi}x_2 + \frac{\phi^2}{2}y_2, |x - y|(h)). \end{array} \tag{3}$$

Then the two half-triangles are given by $\triangle(x', w', z')$ and $\triangle(z', w', y')$, again sharing side $(w', z')$.

Given these definitions, it is a straightforward exercise to show that when $a_1$ and $o_1$ are properly dimensioned acute and obtuse triangles, e.g., $a_1((0, 0), (\phi \cos 72°, \phi \sin 72°), (1, 0))$, $o_1((0, 0), (\frac{1}{\phi} \cos 36°, \frac{1}{\phi} \sin 36°), (1, 0))$, the sides of the half-triangles are in the ratio $1 : \sqrt{3} : 2$, so that the resulting 3D tile triangles are indeed equilateral triangles.

The existence of the Pentasia surface and its relation to the kite-dart tiling leads naturally to the question: is there a corresponding 3D surface based on the rhomb tiling that can be had by lofting each triangle of the rhomb tiling into a triangle pair? There is.

In fact, there is a family of such surfaces for the Penrose rhomb tiling (as there is also a family of surfaces analogous to Pentasia for the kite-dart tiling). Clearly, we could scale the entire 3D tiling by an arbitrary factor in the vertical direction and still arrive at a continuous 3D surface composed of kite-like and dart-like triangle pairs. What makes the particular scaling of Pentasia significant is that for this vertical scale, the lengths in 3D of all edges are the same, i.e., the edges of the 3D tiles form skew rhombii. For other vertical scalings, they would not.

There is another degree of freedom to play with. In the 2D kite-dart tiling, the kite is made up of mirror-image pairs that mate along edge $(y, z)$. In both the 3D kite and dart, the point $w'$ could be located anywhere in the vertical plane containing points $y$ and $x$ and the tiles would still form a continuous surface with all kite-like surface units and all dart-like surface units, respectively, congruent. In the most general case where each planar tile is elevated into four triangles (two of which are the mirror image of the other), the 3D tile is going to be some form of a 4-sided pyramid whose base is a skew rhombus (for the Pentasia scaling factor; a skew kite, in general). For Pentasia, we have chosen the vertical scale and position of $w'$ so that the skew-kite-based 4-side pyramid is simply a folded rhombus, and

not only that: it is the *same* rhombus for the two tiles, differing only in fold angle and orientation.

With that as background, we now turn our attention to the rhomb tiling. If we stipulate the same requirements, that the edges in 3D are all the same length and that the 3D tiles are folded from the same rhombus, differing only in fold angle, we find the 3D tiling shown in Figure 10. This surface has not (to our knowledge) been described before, and so we dub it "Rhombonia".

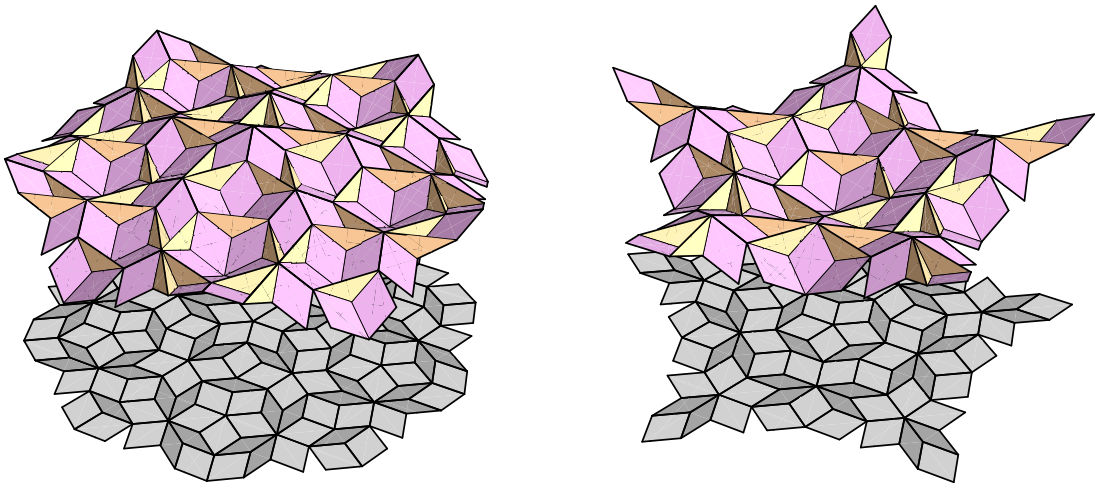

Figure 10: Left: the Bump of the Sun. Right: the Star Dimple.

Rhombonia is noticeably flatter than Pentasia, so we have chosen somewhat more subdued names for the fivefold-symmetric features in in Figure 10. It has one elegant feature of interest: the 3D version of the fat rhomb tile is planar, i.e., not folded at all. The 3D version of the skinny rhomb tile is the same rhombus, folded along its longer diagonal. And, most elegantly of all, the ratio of the two diagonals of this rhombus is $\phi$, the golden ratio making yet another appearance.

To create the Rhombonian surface, we define 4-component triangles $a_4(x, y, z, h)$ and $o_4(x, y, z, h)$ that correspond to the planar triangles $a_2(x, y, z)$ and $o_2(x, y, z)$ of the planar rhomb tiling. The surface triangles are then given as follows.

For the acute triangle $a_4(x, y, z, h)$, we define four vertices

$$\begin{array}{rcl} x' & = & (x_1, x_2, (\frac{\phi}{2} - 1)|y - z|(h)), \\ y' & = & (y_1, y_2, (\frac{\phi}{2} - 1)|y - z|(h - 1 - \phi)), \\ z' & = & (z_1, z_2, (\frac{\phi}{2} - 1)|y - z|(h)), \\ w' & = & (\frac{1}{2}x_1 + \frac{1}{2}y_1, \frac{1}{2}x_2 + \frac{1}{2}y_2, (\frac{\phi}{2} - 1)|y - z|(h)). \end{array} \tag{4}$$

Then the two half-triangles are given by $\triangle(y', z', w')$ and $\triangle(w', x', y')$, sharing side $(w', z')$.

For the obtuse triangle $o_4(x, y, z, h)$, we define the four vertices

$$\begin{array}{rcl} x' & = & (x_1, x_2, (\frac{\phi}{2} - 1)|y - z|(h - 1 - \phi)), \\ y' & = & (y_1, y_2, (\frac{\phi}{2} - 1)|y - z|(h)), \\ z' & = & (z_1, z_2, (\frac{\phi}{2} - 1)|y - z|(h + 1 + \phi)), \\ w' & = & (\frac{1}{2}x_1 + \frac{1}{2}y_1, \frac{1}{2}x_2 + \frac{1}{2}y_2, (\frac{\phi}{2} - 1)|y - z|(h + 1)). \end{array} \tag{5}$$

Then the two half-triangles are given by $\triangle(y', z', z')$ and $\triangle(w', x', y')$, again sharing side $(y', z')$.

The elevated half-triangle pairs are illustrated over their corresponding planar half-triangles in Figure 11.

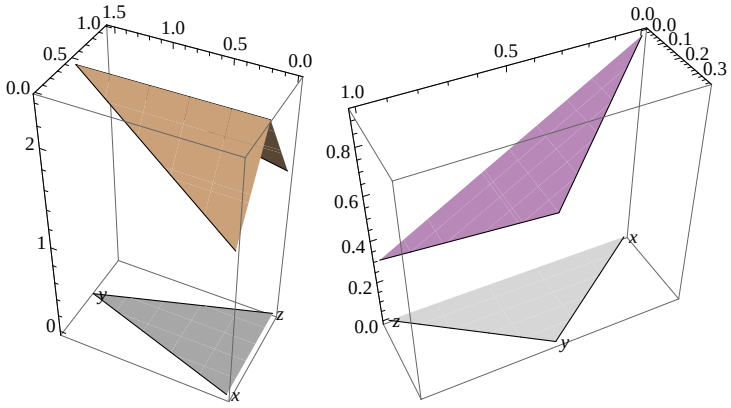


Figure 11: Left: Planar acute triangle $a_2(x, y, z)$ and the 3D triangle pair with specifier $a_4(x, y, z, \phi)$. Right: Planar obtuse triangle $o_2(x, y, z)$ and the 3D triangle pair with specifier $o_4(x, y, z, \phi - 1)$.

Given the coordinates above, it is, again, a straightforward exercise to verify that the the two 3D rhombii do indeed have the same major and minor diagonals. Full 3D tiles are illustrated in Figure 12.

As noted earlier, in both 3D tilings, the position of the point $w'$ (for each tile) is quite arbitrary; it may be chosen anywhere in a vertical plane. In fact, there is considerable freedom in choosing the shape of the elevated surface. One could draw an arbitrary curved line from $x'$ to $y'$ (for the 3D kite-dart tiling) and from $x'$ to $z'$ (for the 3D rhomb tiling) in the vertical plane and any closed surface taking in that line plus the other two lines would

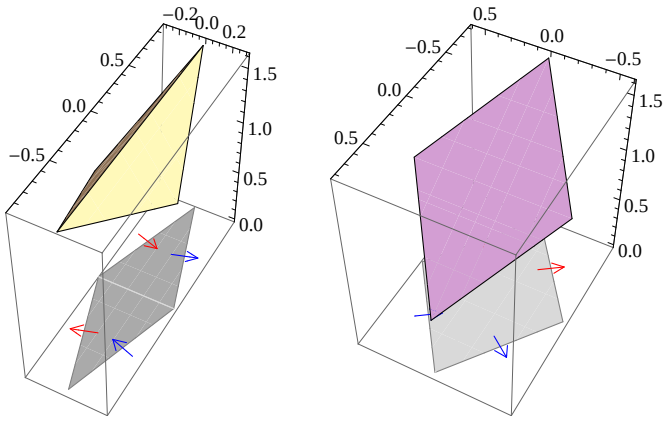


Figure 12: Left: a skinny-rhomb-like triangle pair above a skinny rhomb tile. Right: a fat-rhomb-like triangle pair above a fat rhomb tile.

form a continuous closed 3D surface for any Penrose tiling. What makes this all work are the relative heights of the three vertices $x', y', z'$, which cannot be chosen independently, but instead, must be chosen to be consistent with the production rules corresponding to deflation. That is, we must be able to deflate a 3D tiling in such a way that not only does the planar shadow of a deflated 3D surface match the corresponding deflated 2D Penrose tiling, but the vertex heights must be chosen so that the tiled edges, oriented in 3D, match up after deflation.

Just as the 2D tilings could be grown arbitrarily large by iterated deflation, we can begin with a simple 3D tiling and grow it by 3D deflation, whose production rules are the following.

$$\begin{array}{rcl} a_3(x,y,z,h) & \mapsto & \{a_4(\frac{1}{\phi}x+\frac{1}{\phi^2}y,z,x,h), o_4(z,\frac{1}{\phi}x+\frac{1}{\phi^2}y,y,h)\}, \\ o_3(x,y,z,h) & \mapsto & \{o_4(x,y,z,h-1)\}, \\ a_4(x,y,z,h) & \mapsto & \{a_3(x,y,z,-h)\}, \\ o_4(x,y,z,h) & \mapsto & \{a_3(y,x,\frac{1}{\phi^2}x+\frac{1}{\phi}z,-h), o_3(z,\frac{1}{\phi^2}x+\frac{1}{\phi}z,y,-h)\}. \end{array} \tag{6}$$

These are the same as the 2D production rules, augmented by appropriate values of the height coordinates to ensure that the edges and vertices of incident triangles coincide at each step of deflation.

If we take any surface through repeated cycles of deflation, any initial local peak will alternate between hills and dales as it cycles through Temple of the Sun → Star Dimple → Star Lake → Bump of the Sun and back, alternating between local maximum and minima of the surface with each pair of deflations. Figure 13 shows such an example of eight successive stages of deflation.

What is not immediately apparent from the alternation is that the kite-dart-like surfaces are roughly similar in topography from one iteration to the next, but they alternate in sign of the $z$-coordinate. We can see this by flipping the sign of selected stages of deflation, or equivalently, by adopting a modified set of production rules as follows. For kite-dart tiles, we use triangles $a_5, o_5$ and for rhomb tilings $a_6, o_6$ with an additional parameter $s$ that takes

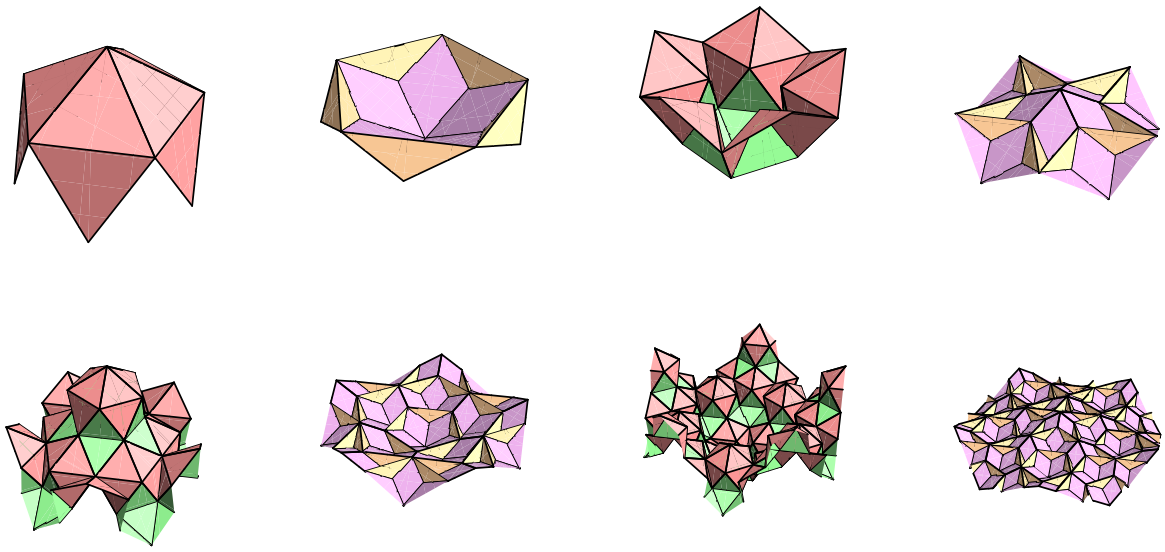

Figure 13: Eight successive stages of deflation of the first Temple of the Sun.

the place of the side lengths in Equations 2–5.

For the acute triangle $a_5(x, y, z, h, s)$,

$$\begin{aligned} x' &= (x_1, x_2, s(h-\phi)), \\ y' &= (y_1, y_2, s(h+1)), \\ z' &= (z_1, z_2, s(h)), \\ w' &= (\tfrac{\phi}{2}x_1 + (1-\tfrac{\phi}{2})y_1, \tfrac{\phi}{2}x_2 + (1-\tfrac{\phi}{2})y_2, s(h)). \end{aligned} \tag{7}$$

For the obtuse triangle $o_5(x, y, z, h, s)$,

$$\begin{aligned} x' &= (x_1, x_2, s(h-1)), \\ y' &= (y_1, y_2, s(h+\phi)), \\ z' &= (z_1, z_2, s(h)), \\ w' &= (\tfrac{-1}{2\phi}x_1 + \tfrac{\phi^2}{2}y_1, \tfrac{-1}{2\phi}x_2 + \tfrac{\phi^2}{2}y_2, s(h)). \end{aligned} \tag{8}$$

For the acute triangle $a_6(x, y, z, h, s)$,

$$\begin{aligned} x' &= (x_1, x_2, (\tfrac{\phi}{2}-1)s(h)), \\ y' &= (y_1, y_2, (\tfrac{\phi}{2}-1)s(h-1-\phi)), \\ z' &= (z_1, z_2, (\tfrac{\phi}{2}-1)s(h)), \\ w' &= (\tfrac{1}{2}x_1 + \tfrac{1}{2}y_1, \tfrac{1}{2}x_2 + \tfrac{1}{2}y_2, (\tfrac{\phi}{2}-1)s(h)). \end{aligned} \tag{9}$$

For the obtuse triangle $o_6(x, y, z, h, s)$,

$$\begin{aligned} x' &= (x_1, x_2, (\tfrac{\phi}{2}-1)s(h-1-\phi)), \\ y' &= (y_1, y_2, (\tfrac{\phi}{2}-1)s(h)), \\ z' &= (z_1, z_2, (\tfrac{\phi}{2}-1)s(h+1+\phi)), \\ w' &= (\tfrac{1}{2}x_1 + \tfrac{1}{2}y_1, \tfrac{1}{2}x_2 + \tfrac{1}{2}y_2, (\tfrac{\phi}{2}-1)s(h+1)). \end{aligned} \tag{10}$$

An initial configuration can then be deflated according to the production rules

$$\begin{array}{rcl} a_5(x,y,z,h,s) & \mapsto & \{a_6(\frac{1}{\phi}x+\frac{1}{\phi^2}y,z,x,h,(1-\frac{\phi}{2})s),o_6(z,\frac{1}{\phi}x+\frac{1}{\phi^2}y,y,h,(1-\frac{\phi}{2})s)\},\\ o_5(x,y,z,h,s) & \mapsto & \{o_6(x,y,z,h-1,(1-\frac{\phi}{2})s)\},\\ a_6(x,y,z,h,s) & \mapsto & \{a_5(x,y,z,-h,-2\phi s)\},\\ o_6(x,y,z,h,s) & \mapsto & \{a_5(y,x,\frac{1}{\phi^2}x+\frac{1}{\phi}z,-h,-2\phi s),o_5(z,\frac{1}{\phi^2}x+\frac{1}{\phi}z,y,-h,-2\phi s)\}. \end{array} \tag{11}$$

With these definitions, successive stages of Pentasia are topographically similar to one another, as are too the (interwoven) successive stages of Rhombonia.

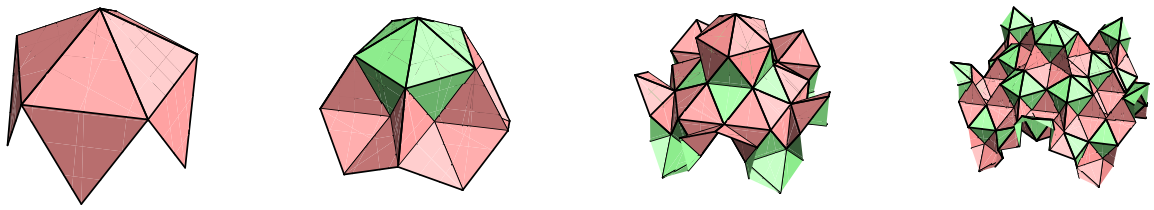

Figure 14: Four successive stages of Pentasia, using the alternate production rules.

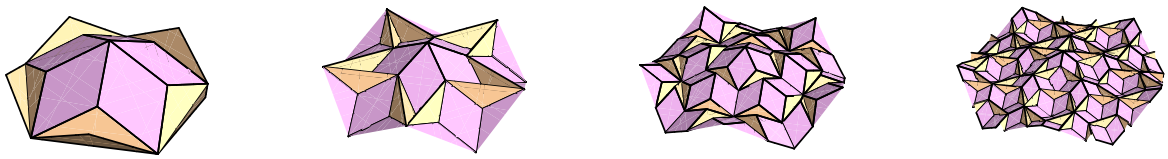

Figure 15: Four successive stages of Rhombonia, using the alternate production rules.

Both Pentasia and Rhombonia are mathematically interesting surfaces due to their connections to the 2D Penrose tiling and, on their own, suggest numerous artistic applications, both for the surfaces themselves and for their generalizations. But the fact that they both can be created from identical units, and *folded* units as well, makes them particularly suggestive of modular origami. And so we now turn to their origami realization.

# Origami Pentasia

The transformation from kites and darts to hypothetical origami units is illustrated in Figure 16 (a)–(d). We begin with the top row, the kite. In (a), we show the kite with matching

arrows. This image can also be considered to be the projection from above of the 3D tile, in which case the stubby corner at the bottom is actually a downward-pointing equilateral triangle. We unfold this triangle (as well as the upper one, which is also tilted relative to the plane of projection), to arrive at the 60°/120° rhombus shown in (b), together with the appropriate matching arrows.

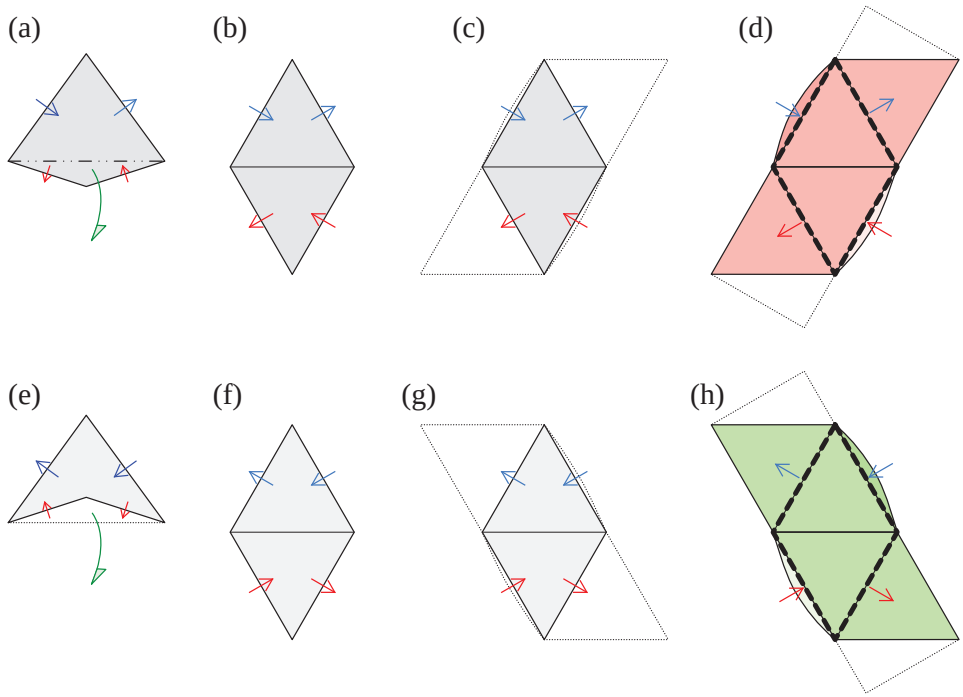


Figure 16: Progression from the kite (top row) and dart (bottom row) to a hypothetical origami unit. (a) The 2D kite (or projection of 3D) tile. (b) The unfolded and flattened tile. (c) Positions of tabs and pockets that are consistent with matching rules. (d) Actual tabs and pockets where both color and gender enforce matching rules. (e)–(h): Same thing for the dart tile.

Now we must create the means of assembling tiles in such a way that matching rules can be enforced. A common way of assembling origami modular structures is to insert tabs into pockets. Since the matching arrows come in opposite-gender pairs, it is a logical choice to create tabs for outgoing arrows and pockets for incoming arrows, as illustrated schematically in subfigure (c) by the dotted lines.

There is also the question of enforcing color-matching of the arrows; let us set that aside for the moment, and focus just on their direction. A minimal hypothetical kite-like unit is illustrated in subfigure (d). We can extend the tab a bit, if we wish, which will give an even more secure lock; the extension is shown by a dotted line at top and bottom, and this extension suggests a strategy on how to realize the unit; more on that in a minute.

Now we turn to the dart tile in Figure 16(e)–(h). We proceed in the same way—it, too, will unfold into a 60°/120° rhomb—but there are two differences to consider. The first is

that even though we end up with a 60° rhombus, the matching arrows on the edges are different than they were for the kite tile. The second is to make sure that when we unfold the overhanging lower triangle (corresponding to the reflex corner of the tile) that we get the arrow direction correct; the red arrow points *into* the tile on the left side, *out of* the tile on the right, and so this arrow direction must be preserved on the unfolded flat rhombus, as in subfigure (f).

And here we note a pleasant coincidence: the flattened dart rhombus is the mirror image of the flattened kite rhombus, including the matching arrows. So this, in turn, means that the dart origami unit can simply be the mirror image of the kite origami unit; other than the mirror reflection, the two units can be folded in exactly the same way.

But how to actually fold units with tabs and pockets in the desired locations?

In the world of modular origami, there are "face units," "edge units,", and "vertex units," which describe structures that, at least topologically, correspond to faces, edges, or vertices, respectively, of the polyhedra that are formed from assemblies of said units. Among the most well-known are several edge units, which include the Sonobe unit [7] and various units by Lewis Simon [18], Robert Neale [13], and Thomas Hull [5], among others. Many of these edge units can be classified as "Zig-Zag units," a nomenclature coined by Hull, whose own Pentahedral-Hexahedral Zig-Zag unit (or PHiZZ unit, as it is commonly known) has been used for many examples of mathematical polyhedra. The PHiZZ unit (and at least one of its inspirations, Robert Neale's Dodecahedron [13]) has a relatively simple folding concept. A strip of paper is pleated in such a way as to give a strip with two extended pockets along its long edges; then ends of the strip are then folded into tabs, and additional diagonal creases are added to define triangular faces.

Author RJL has previously used this approach to create a unit suitable for folding elevated deltahedra (polyhedra with equilateral triangular faces replaced by regular tetrahedra) [9]. The basic unit for folding any modular origami deltahedron is a 60°/120° rhombus with tabs and pockets alternating around the form; it contains the geometry, tabs, and pockets required for an origami implementation of Pentasia.

There are eight possible matings of units that obey both arrow direction (enforced by tab versus pocket) and color (enforced, for the moment, by labeling each unit with the appropriate colored arrow). Four of the options are shown in Figure 18; the others follow in the same fashion.

Figures 20 and 18 show the units as flattened, but all of the creases that outline equilateral triangles should have nonzero dihedral angle folds in them to give them the proper 3D form. We leave as an exercise for the reader the folding of a collection of units and their assembly into a portion of the surface of Pentasia.

An aesthetic deficiency of the above is the need to keep track of whether a given tab or arrow is "red" or "blue" to enforce matching rules. Since origami is traditionally folded from two-colored paper, it would be desirable to create units in which the colors of the two paper sides enforced the color matching of the arrows. This is, in fact, achievable, by adding one extra step to the folding sequence of Figure 17, as shown in Figure 19. As it turns out, the original unit has sufficient extra paper that it is possible to modify it to implement the

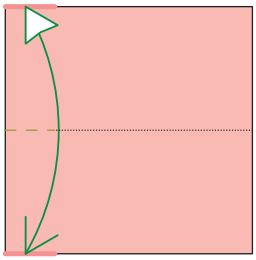

**1.** Begin with a square, colored side up. Fold in half vertically and unfold, making a pinch at the left.

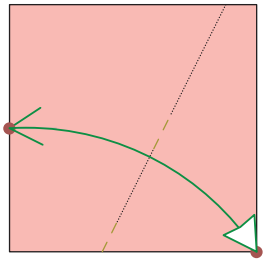

**2.** Fold the bottom left corner to the mark you just made, creasing as lightly as possible.

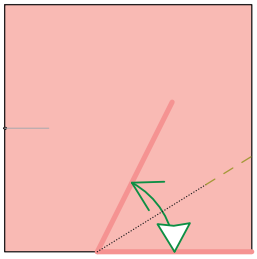

**3.** Fold and unfold along an angle bisector, making a pinch along the right edge.

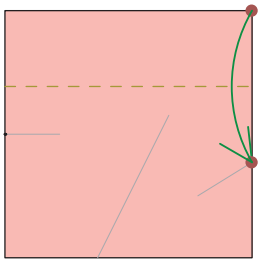

**4.** Fold the top left corner down to the crease intersection.

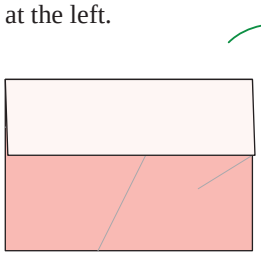

**5.** Turn the paper over.

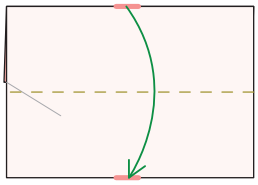

**6.** Fold the top folded edge down to the raw bottom edge.

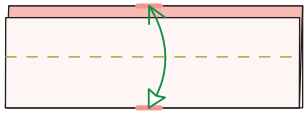

**7.** Fold the bottom folded edge (but not the raw edge behind it) up to the top and unfold.

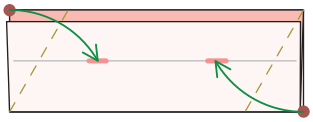

**8.** Fold the top left corner and the bottom right corner to the crease you just made.

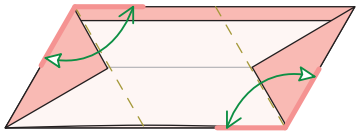

**9.** Fold and unfold along angle bisectors.

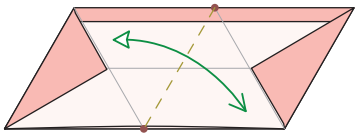

**10.** Fold and unfold, connecting the crease intersections.

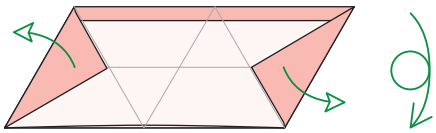

**11.** Unfold the two corners and turn the paper over from top to bottom.

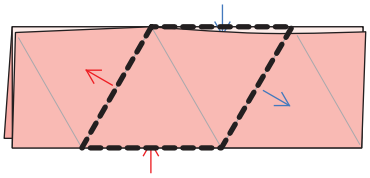

**12.** The finished kite-like unit. The exposed part of the surface is outlined.

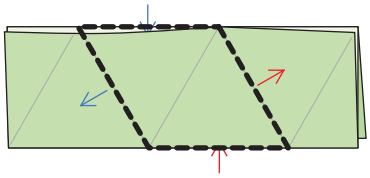

**13.** Dart-like units are mirror images of kite-like units.

Figure 17: Folding instructions for the 3D Penrose tiling origami unit.

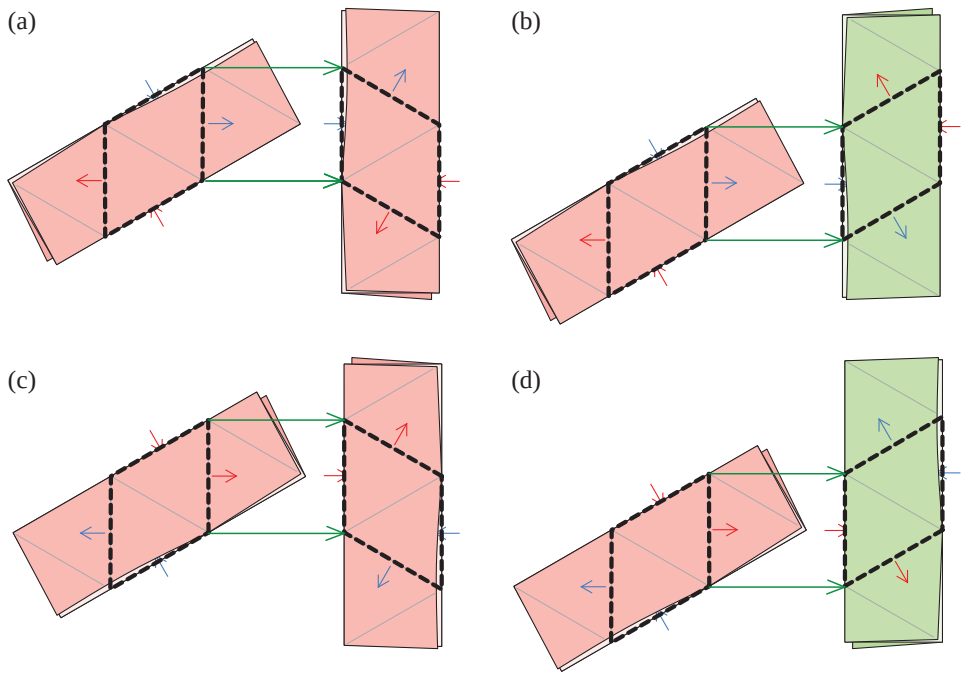


Figure 18: Allowed tab-slot matings for the origami units.

desired color change, albeit with a slight reduction in security of the locking mechanism.

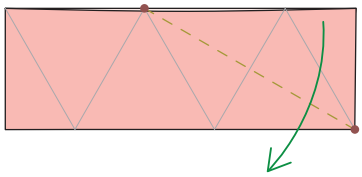

**12.** Fold one layer of paper down along a crease between the two points.

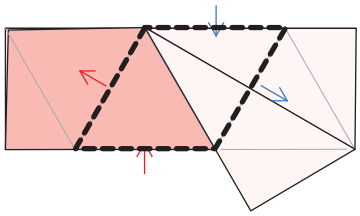

**13.** The finished kite-like unit.

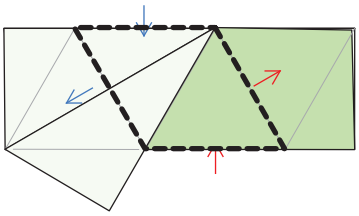

**14.** Dart-like units are mirror images of kite-like units.

Figure 19: Modification to make a two-color unit where paper color matches arrow color in enforcing the matching rules.

This sequence does not precisely give the ideal rectangular pattern; folding a layer down to create the white layer on one side changes the slot in such a way that it reduces the overlap between tabs and slots. We therefore keep the extra paper that pokes out beyond the rectangular strip as it will provide a corresponding increase in layer overlap (albeit in a different location) that will maintain the security of the lock. The tabs and slots for the two types of units are illustrated in Figure 20.

The matching rules for these two types of tile mirror the matching rules on their corresponding 2D Penrose tiles. In brief: colored tabs may only go into colored-edge slots, and white tabs may only go into white-edge slots. Between green and red units, there are a total

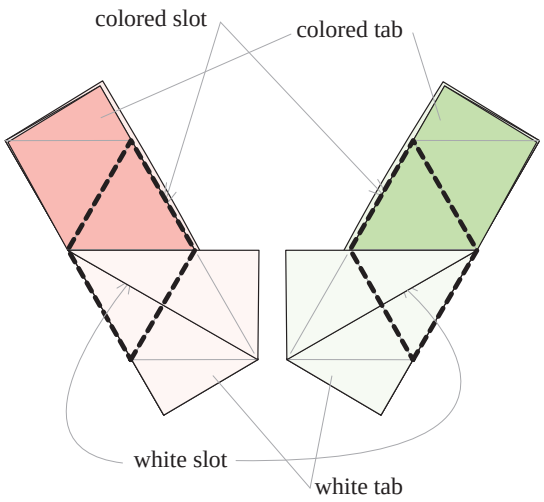


Figure 20: White and colored tabs and slots for the two-colored kite-like (red) and dart-like (green) origami units, which are mirror images of each other. The surface rhombii are outlined in heavy dashed line.

of eight possible allowed matings. Four of those are shown in Figure 21; the other four are the same under simultaneous mirror image and red$\longleftrightarrow$green color reversal.

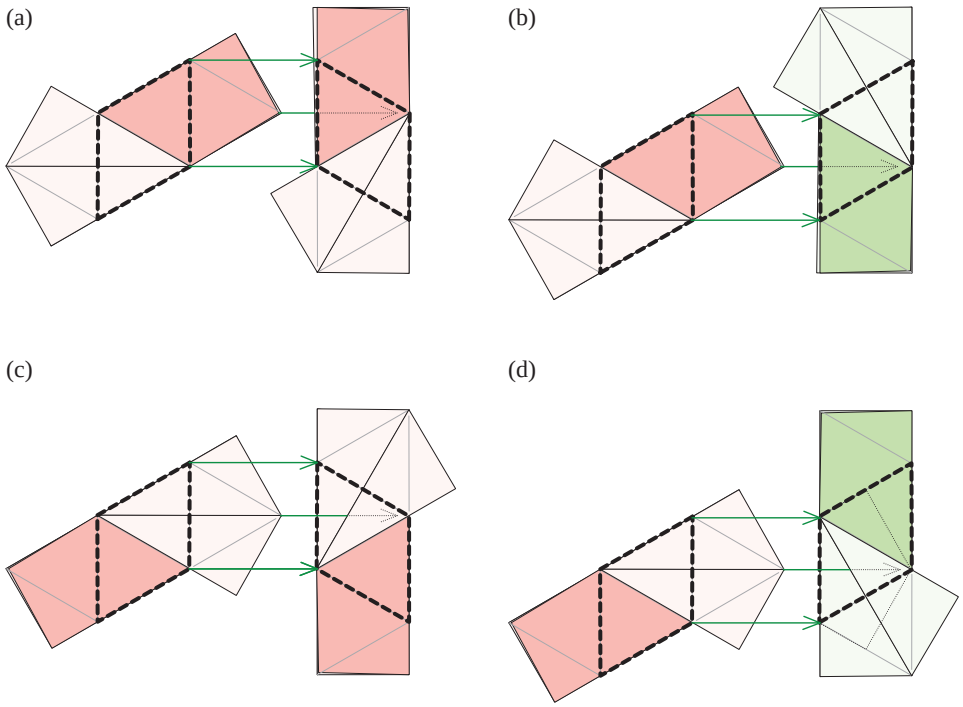


Figure 21: Allowed tab-slot matings for the two-color origami units.

The choice of which type of unit to fold boils down to aesthetics and what one is after:

the solid-color units emphasize the kite-dart pattern of the projection; the multi-colored units emphasize the matching rules. (The locking mechanism of the solid-color unit is also a bit more secure; even with that, one may wish to use a spot of glue or two when assembling the units.)

Whichever one folds, having designed an origami implementation of Pentasia, a logical next step is to consider whether an origami version of Rhombonia would be similarly possible. In principle, it's definitely possible. In practice, though, a different strategy would be required. Figure 22 shows why.

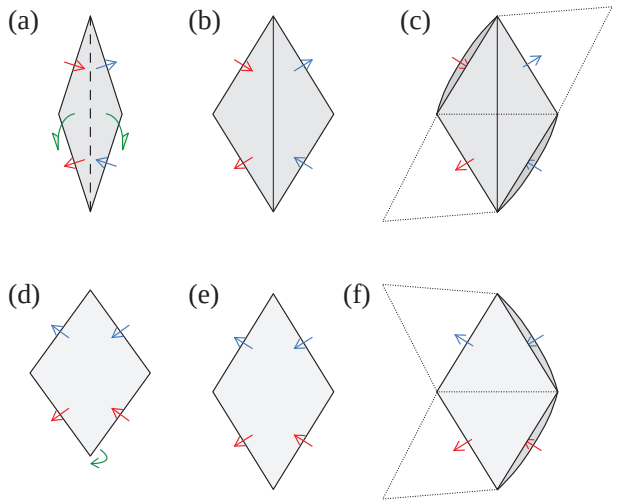


Figure 22: Progression from the skinny rhomb (top) and fat rhomb (bottom) toward a hypothetical origami unit. (a,d) The 2D (or projection of 3D) tiles. (b,e) The unfolded and flattened tiles. (c,f) Required positions of tabs and pockets for matching.

As before, we unfold each rhomb tile into a flat rhombus. (The fat rhomb tile is already planar, but tilted; we need only to rotate it into the plane.) Both rhombii have their diagonals in the ratio $\phi$, which makes them both 63.43°/116.57° rhombuses. These are not particularly "nice" angles. The real problem arises when we strive to convert tabs and pockets into matching rules. To use a zig-zag approach, we need two parallel pockets on opposite sides of the unit. The skinny rhomb unit clearly calls for that. However, the fat rhomb unit would require having pockets on two *adjacent* sides, so the zig-zag unit approach can't be used here.

We could, of course, reverse the directions of the red arrows on both units, which would turn the fat rhombus into a zig-zag-able unit; but then the pockets would be misplaced on the skinny rhomb unit.

The conclusion is not that an origami version of Rhombonia is impossible; any connected shape is possible with origami [2, p. 232], whether single-sheet or modular. But the particular arrangement of the matching conditions of Pentasia, combined with the symmetry of the 60°/120° rhombus, gives rise to a simple and elegant origami folding unit.

While the complete (and thus infinite) tiling is beyond even the most avid folder, one can use the Temple of the Sun or Star Lake as the starting point for as large a modular

construction as one could desire. As a practical verification of the construction, Figure 23 shows a photograph of a folded portion of the Temple of the Sun folded from the solid-color units, 165 kite-like units (brown) and 100 dart-like units (gray).

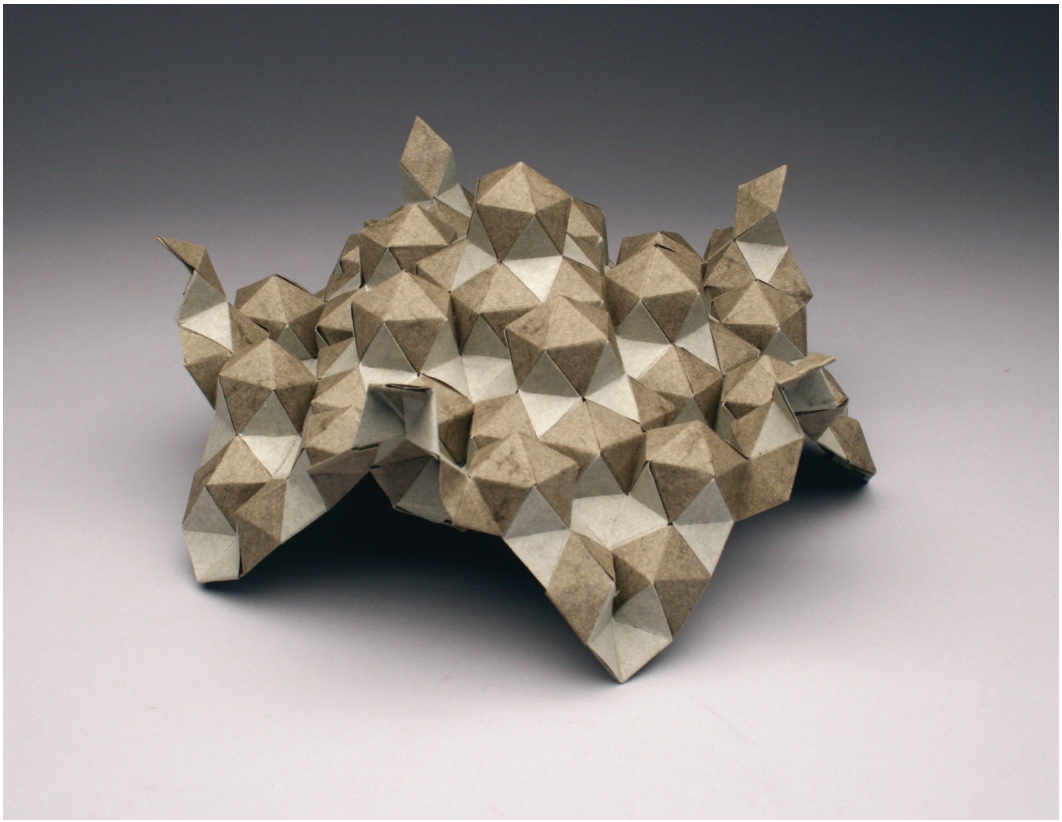

Figure 23: A folded Pentasian Temple of the Sun, from 165 kite-like units and 100 dart-like units.

# Conclusions

In summary, we have provided a description of two elegant surfaces based on the Penrose tiling: Pentasia, composed of folded 60°/120° rhombs, and Rhombonia, composed of 63.43°/116.57° rhombs (some folded, some not). Both surfaces are elevations of planar Penrose tilings: the former from a kite-dart tiling, the latter from the rhomb tiling. We showed how arbitrarily large sections of either surface can be constructed by deflation and gave explicit production rules for both. Should the reader wish to explore these surfaces further, the authors have created our own *Mathematica*™ package, *PenroseTiles3D* [8], which we used for many of the figures in this paper, and which may be freely downloaded from the link in the references.

We note that both surfaces can be readily generalized to surfaces of more complex topography, which offers great artistic potential. As a first example of this potential, we presented

a modular origami implementation of the Pentasia surface. Such a figure offers aesthetic, mathematical, and pedagogical appeal, as an illustration of the wondrous variety of forms residing at the intersection of origami, art, and mathematics.

## Acknowledgements

The authors would like to thank John Conway for introducing the surface and for subsequent fruitful discussions, Lyman Hurd, whose *Mathematica*™ package *PenroseTiles* provided a springboard for our own explorations, and to thank and acknowledge the late Thomas Rodgers for organizing the *Gathering for Gardner* meetings that brought the authors together, and of course, the late Martin Gardner, for inspiring us in our own individual ways to travel this path.

## References

[1] N. G. de Bruijn. Algebraic theory of penrose's non-periodic tilings of the plane I. *Proceedings of the Koninklijke Nederlandse Akademie van Wetenschappen Series A*, 84(1):39–52, 1981.

[2] Erik D. Demaine and Joseph O'Rourke. *Geometric Folding Algorithms: Linkages, Origami, Polyhedra*. Cambridge University Press, 2007.

[3] Tomoko Fuse. *Unit Origami: Multidimensional Transformations*. Japan Publications, Tokyo, Japan, 1990.

[4] Martin Gardner. *Penrose Tiles to Trapdoor Ciphers: And the Return of Dr. Matix*. W. H. Freeman & Co., 1988.

[5] Thomas Hull. *Project Origami*. A K Peters Ltd., 2006.

[6] Lyman Hurd. Penrose tiles. `http://library.wolfram.com/infocenter/MathSource/595/`, retrieved 2012-04-09, 2010.

[7] Kunihiko Kasahara and Toshie Takahama. *Origami For the Connoisseur*. Japan Publications, Tokyo, Japan, 1987.

[8] Robert J. Lang. Penrose tiles 3D. `http://www.langorigami.com/science/computational/pentasia/PenroseTiles3D.nb`, retrieved 2012-07-30, 2010.

[9] Robert J. Lang. Modular origami: the DeZZ unit. `http://origamiusa.org/thefold010_lang_dezz_unit`, retrieved 2012-07-30, 2012.

[10] Jeannine Mosely. Business card menger sponge exhibit. `http://theiff.org/oexhibits/menger02.html`, retrieved 2012-04-04, 2006.

[11] Jeannine Mosely. The mosely snowflake sponge. http://www.theiff.org/exhibits/sponge.html, retrieved 2012-04-04, 2012.

[12] Meenakshi Mukerji. *Marvelous Modular Origami*. A K Peters Ltd., 2007.

[13] Robert E. Neale and Thomas Hull. *Origami Plain and Simple*. St. Martin's Press, 1994.

[14] Roger Penrose. Pentaplexity. *Eureka*, 39:16–22, 1978.

[15] Roger Penrose. Pentaplexity. *The Mathematical Intelligencer*, 2:32–37, 1979.

[16] Anne Preston. You were in heaven. http://www.flysfo.com/web/page/about/news/pressres/art.html, retrieved 2012-04-14, 2000.

[17] Przemyslaw Prusinkiewicz, Aristid Lindenmayer, J. S. Hanan, and F.D. Fracchia. *The Algorithmic Beauty of Plants*. Springer, 1991.

[18] Lewis Simon, Bennett Arnstein, and Rona Gurkewitz. *Modular Origami Polyhedra*. Dover Publications, Mineola, New York, 1999.